Available online at www.sciencedirect.com
ScienceDirect
International Journal of Heat and Mass Transfer 51 (2008) 1793–1803
International Journal of HEAT and MASS TRANSFER
www.elsevier.com/locate/ijhmt

Effectiveness–NTU relation for packed bed liquid desiccant–air contact systems with a double film model for heat and mass transfer

Cheng Qin Ren *

College of Mechanical and Automotive Engineering, Hunan University, Changsha 410082, China

Received 17 May 2006; received in revised form 8 June 2007
Available online 24 September 2007

Abstract

One-dimensional models were usually utilized to describe the coupled heat and mass transfer processes in packed bed liquid desiccant–air contact systems. In this paper, a double film model was utilized for both parallel and countercurrent flow configurations. The model considered the effects of non-unity values of Lewis factor, unequal effective heat and mass transfer areas, liquid phase heat and mass transfer resistances, changes in solution mass flow rate and concentration. Within the relatively narrow range of operating conditions usually encountered in a specified application, a linear approximation was made to find out the dependence of equilibrium humidity ratio on solution temperature and concentration. Constant approximations of some properties and coefficients were further made to render the coupled equations linear. The original differential equations were rearranged and an analytical solution was developed for a set of newly defined parameters. Analytical expressions for the tower efficiency and other effectiveness values were further developed based on the analytical solution. Comparisons were made between analytical results and numerical integration of the original differential equations and the agreement was found to be quite satisfactory.

Keywords: Liquid desiccant–air contact systems; Double film heat and mass transfer model; Analytical solution; Effectiveness expressions

1. Introduction

Liquid desiccant cooling system driven by solar energy or other heat sources was emerged as a potential alternative or as a supplement to conventional vapor compression systems for cooling and air conditioning. Dehumidification and regeneration are the key processes.

One-dimensional models were frequently utilized to describe the heat and mass transfer processes in packed bed liquid desiccant–air contact systems with different approximations concerning the individual phase heat and mass transfer resistances. Factor and Grossman [1] developed a differential model for a test column using LiBr solutions. The interface temperature and concentration were assumed to be the bulk liquid temperature and concentration, respectively. Overall heat and mass transfer coefficients were utilized. The model was validated with experimental results for a column packed with ceramic Intalox saddles. Such kind of models was also utilized by some other research workers [2,3] in studying the performance of dehumidifiers and regenerators. Neglecting the liquid phase heat transfer resistance and using individual phase mass transfer coefficients, Gandhidasan et al. [4] simulated the performance of a dehumidification tower using packings of Ceramic 2 in Rashing rings and aqueous $CaCl_2$ solution. It was found that, if liquid phase mass transfer resistance was ignored, the packed height would be underestimated by about 10–20% depending on the concentration of the desiccant used. Oberg and Goswami [5] and Martin and Goswami [6] also included the liquid phase mass transfer resistance in their finite difference model to study the performance of adiabatic absorption and regeneration with TEG, respectively. Gas and liquid phase mass transfer coefficients were calculated using the empirical correlations by Onda et al. [7]. Gas phase heat transfer coefficient was

* Tel.: +86 13874886953; fax: +86 731 8711911.
E-mail address: renchengqin@163.com

0017-9310/$ - see front matter © 2007 Elsevier Ltd. All rights reserved.
doi:10.1016/j.ijheatmasstransfer.2007.07.038

Nomenclature

a, a_M	effective specific interfacial areas for contact of a gas with liquid for heat and mass transfer, respectively (m^2/m^3)
a_{11}–a_{22}	elements of coefficients matrix defined in Eq. (23)
A	coefficients matrix first introduced in Eq. (21)
B_0–B_3	coefficients first appeared in Eqs. (8)–(10) and (23), respectively
C, C_p	specific heat capacities (kJ/kmol °C)
C^*	air to solution heat capacity rate ratio
E_t, E_x	average or derivative slopes of equilibrium humidity ratio with respect to temperature and concentration, respectively
G	dry air mass flow rate (kmol/s)
h	specific enthalpy (kJ/kmol)
h_a	specific enthalpy of moist air $h_a = (C_{pa} + Y_a C_{pv}) t_a + Y_a h_{fg,0}$ (kJ/kmol)
$h_{fg,0}$	evaporation heat of water at reference temperature (0 °C) (kJ/kmol)
h_v	specific enthalpy of water vapor $h_{fg,0} + C_{pv} t_v$ (kJ/kmol)
h_G	gas phase heat transfer coefficient (kW/m^3 °C)
h_L	liquid phase heat transfer coefficient (kW/m^3 °C)
$\hat{h}_w$	partial enthalpy of water in solution $\hat{h}_w = h_L + (1 - x_L)\frac{\partial h_L}{\partial x_L}$ (kJ/kmol)
$h_{s,I}$	heat of absorption at interface condition $h_{s,I} = h_{v,I} - \hat{h}_{w,I}$ (kJ/kmol)
$\bar{h}_{fg}$	a normalized heat of evaporation $h_{fg,0}/C_{pa}$ (°C)
k_Y, k_x	gas and liquid phase mass transfer coefficients, respectively (kmol/m^2 s)
K_1, K_2	coefficients defined by Eq. (29)
L	mass flow rate of solution (kmol/s)
Le_f	Lewis factor
m_R	air to solution mass flow rate ratio
M	molecular weight
NTU	number of heat transfer units
Pr	Prandtl number
P_1–P_4	parameters first appeared in Eqs. (14) and (15), respectively
Q	sensible heat transferred
R_{cv}	water vapor to dry air specific heat capacity ratio
R_h	ratio of gas-to-liquid phase heat transfer coefficients
R_k	ratio of gas-to-liquid phase mass transfer coefficients
Sc	Schmidt number
S_ϑ	coefficient in Eq. (23)
t	temperature (°C)
V	volume of packed column (m^3)
W	mass of water species transferred
x	mole fraction of water in solution (kmol/kmol)
Y	humidity ratio (kmol/kmol(a), or mol/mol(a))
Y	function variable vector defined by Eq. (22)

Greek symbols

Δ	change of or difference between parameters
β_1–β_5	coefficients defined by Eqs. (49)–(52), respectively
δ_a	flow direction indicator, "+1" for counterflow and "−1" for parallel flow
ε	effectiveness
γ	coefficient defined by Eq. (61)
λ_1, λ_2	roots of the characteristic equation
ϑ	dimensionless temperatures $t/\bar{h}_{fg}$
σ	ratio of mass transfer area to the effective heat transfer area
ξ	mass fraction of desiccant in solution (wt% salt)
φ, ψ	newly defined variables in Eq. (32)

Subscripts

a	of or in bulk air
av	average
e	of air in equilibrium with desiccant solution
i	inlet
I	of or at interface
L	of or in bulk solution
o	outlet
v	water vapor
x	local position
T	top position

found by applying the heat and mass transfer analogy. Model predictions were found to be in good agreement with the experimental results. Further, Fumo and Goswami [8] made modifications to account for the higher surface tension of LiCl and higher water concentration in brines as compared to water concentration in TEG. A correction factor was used in their model to describe the reduction of area for mass transfer in the contact column. Gas phase heat transfer coefficient was also determined from known mass transfer coefficient by applying the heat and mass transfer analogy. The model was used to predict experimental findings and the results of comparison were satisfactory.

Different assumptions concerning the individual phase heat and mass transfer resistances in the liquid desiccant air contact systems are appropriate for different packing materials and operating conditions.

Effects of liquid phase heat and mass transfer resistances may sometimes be considered as negligible in liquid desiccant air contact systems with random packings.

Gandhidasan et al. and Ertas et al. [9,10] calculated and correlated both liquid and gas phase heat and mass transfer coefficients for random packing materials and $CaCl_2$, LiCl and CELD solutions using method presented in Ref. [11]. For the specified range of operating conditions, numerical calculation gives that the ratios of gas-to-liquid phase heat transfer coefficients (R_h) are very small, approximately among 0.0028–0.022. For simplification, the effects of liquid phase heat transfer resistances can approximately be neglected. For the same packing materials and operating conditions, the ratios of gas-to-liquid phase mass transfer coefficients (R_k) are among 0.025–0.4682 with large ratio values corresponding to the high gas flow rate and low liquid flow rate operating conditions. Because water is easily soluble in above desiccant solutions, the effects of liquid phase mass transfer resistances can sometimes be neglected too for small ratio values, depending on the operating conditions and the errors to be allowed in engineering calculations. The reason can be given as follows. The relative role of liquid phase mass transfer resistance will be $E_x R_k$, where $E_x = \frac{\partial Y_e}{\partial x}$ is the slope of equilibrium humidity ratio with respect to desiccant concentration (This will be demonstrated in later discussions). Further, E_x is usually small for the easily soluble desiccant solutions. This value will be in the order of 0.1–0.6 mol/mol except for much high solution temperature conditions, but is usually less than 1 in practical applications. Thus, the relative importance of the liquid phase mass transfer resistances will be smaller than that represented by the pure mass transfer coefficients ratios. In consequence, the effects of liquid phase mass transfer resistances can sometimes be neglected too, especially when overall gas phase mass transfer coefficients are utilized. However, for general application purposes and accuracy in simulation, liquid phase mass transfer resistances should better be considered in model equations.

Gas phase-controlled model were frequently utilized in experimental investigations on heat and mass transfer performances of liquid desiccant air contact systems, but there were still some experimental investigations that show that liquid phase heat and mass transfer resistances cannot be neglected. Due to the complications in analyzing the coupled heat and mass transfer processes, it is very difficult to separate liquid phase heat and mass transfer resistances from those of gas phase in a single experimental investigation. Arbitrary assumptions were usually found in experimental investigations. Under the gas phase-controlled assumptions, Chung et al. [12–14] performed experiments to measure the gas-phase heat transfer coefficients and overall gas-phase mass transfer coefficients of packed bed absorbers with random (5/8 in. polypropylene Flexi rings and 1/2 in. ceramic Berl saddles) and structured (cross corrugated cellulose and polyvinyl chloride) packings and LiCl solutions. The values of mass transfer coefficients were among 0.0617–0.227 kmol/(m^3 s). However, the interface temperature was assumed as the arithmetic average of the bulk gas and liquid temperatures and the heat and mass transfer correlations did not necessarily follow the Colburn analogy [12]. In experimental investigations, the superficial mass velocities of liquid solutions were about 8.7–15.2 kg/(m^2 s). For small liquid flow rate conditions, the situations may be quite different. Potnis and Lenz [15] showed through Wilson plots of the experimental data of evaporation and condensation rates for the regenerator and the dehumidifier, respectively, that gas phase mass transfer resistance was negligible compared to the liquid phase mass transfer resistance. The superficial mass velocities of liquid solutions were about 1–3 kg/(m^2 s). Overall liquid phase mass transfer coefficients for the structured packings (Munters CELDEK) (about 0.014–0.04 mol/(m^2 s)) were about 30–40 times less than those for random packing (Polypropylene Tripack) (about 0.48–2 mol/(m^2 s)). The overall mass transfer resistances for structured packings are also very large in comparison with those found by Chung et al. [12]. This really indicated that liquid phase mass transfer resistance played a very important role in these situations, at least for structured packings. From heat and mass transfer analogy, it may also be reasonable to expect a non-negligible effect of liquid phase heat transfer resistance here, if accurate simulation is concerned.

It is possible to get a more comprehensive understanding of the mechanism of the complicated heat and mass transfer processes in liquid desiccant air contact systems from other absorption or desorption processes with approximate diffusivities of transferred species in mixtures. Based on the correlations developed by Bravo et al. [16,17] and Rocha et al. [18,19], Al-Farayedhi et al. evaluated theoretically the heat and mass transfer coefficients in a gauze-type structured packing air dehumidifier operating with liquid desiccant. The gas-side mass transfer coefficient was evaluated according to the wetted-wall relationship, but the liquid-side mass transfer coefficient was evaluated according to the penetration theory where the exposure time was calculated based on the corrugation side length as the flow length. Heat transfer coefficients for both the gas and liquid side were evaluated according to the heat–mass transfer analogy. The evaluated volumetric mass transfer coefficient for air was approximately among 0.125–0.19 kmol/(m^3 s) and the evaluated F-type volumetric mass transfer coefficient for liquid was approximately among 0.4–1.8 kmol/(m^3 s). These results show that the liquid-side mass transfer resistances are much smaller than the gas-side mass transfer resistances. However, this evaluation may greatly overestimate the liquid-side mass transfer coefficients. Weiland and Ahlgren [21] performed experimental studies on the mass transfer characteristics of some structured packings (Goodloe packings and ChemPro's Montz A2 packing). Absorption of SO_2 from air into aqueous caustic soda was used to determine $k_G a$ because this is a completely gas phase-controlled process. Interfacial areas were measured using CO_2 absorption into dilute NaOH from nominal 2% CO_2 in air under conditions of pseudo-first-order reaction. The liquid film coefficient $k_L a$ was found from rates of absorption of CO_2 into sodium

carbonate/bicarbonate buffer solutions. Experimental results were compared with the prediction by the correlation of Bravo et al. [16] and showed that Bravo's correlations underestimated the gas-side mass transfer coefficients and greatly overestimated the liquid-side mass transfer coefficients. The reason may be withdrawn from the experimental interpretation by Brunazzi and Paglianti [22] for how the column height influences the height of a transfer unit. In their investigations, overall liquid phase mass transfer coefficients were measured through experiments of desorption of CO_2 from water into air. This is nearly a liquid phase-controlled process because CO_2 is sparingly soluble in water. Thus the overall liquid phase mass transfer coefficients can be considered identically as the individual liquid phase mass transfer coefficients. Brunazzi and Paglianti found that in a log–log plot the relation between the liquid Sherwood number ($Sh_L = k_L d/D_L$) and the inverse of the Graetz number ($Gz = Re_L Sc_L \delta/H$) is a straight line. Here H is proportional to the column height Z, that is,$H = Z/\sin\alpha$. The Sherwood number increases with the increasing Graetz number. This result is in consistent with the finding made by Nawrocki and Chuang [23] that flow distance is considerably important on mass transfer of absorption of CO_2 into stable rivulets and with the assumption of only partial mixing occurred at corrugation junctions. Finally, Brunazzi and Paglianti's model predicted their own experimental results and Weiland and Ahlgren's experimental results fairly well. The above findings also indicate that using corrugation side length as the flow length in calculating the exposure time will let the penetration theory greatly overestimate the liquid phase mass transfer coefficients. Proofs for that both gas and liquid phase heat and mass transfer resistances may play important roles with random packings may be withdrawn from the supporting information of a statistical analysis of experimental data from a great number of source literatures [24], where the operating conditions is very similar to those found in liquid desiccant air contact systems.

In conclusion, for general application purposes and for accurate simulation and analysis, the effects of both liquid phase heat and mass transfer resistances should be considered in modelling and the Lewis number and the surface wettability were not necessary to be unity.

Functional relationships for the performances of dehumidifiers and regenerators were also investigated by many research workers. Expressions correlating the independent variables to the rates of vaporization in regenerators and the rates of condensation in dehumidifiers were obtained by statistical analysis of numerical or experimental results [25,26]. Semi-empirical expressions for effectiveness of heat and mass transfer processes were also presented by fitting them to the simulation or experimental results [27–29]. However, the validity of these correlations was found to be restricted to the type of equipments and operating conditions investigated. Though some correlations were based on the dimensionless groups obtained from dimensional analysis using Buckingham-Pi theorem, the theorem itself could not help find out the exact functional forms of the correlations. Thus, accuracy will inevitably be compromised for broader ranges of validity and/or simplicity of the expressions. Charts of humidity and enthalpy effectiveness obtained from finite difference model as a function of design variables using calcium chloride solution as the desiccant were presented by Elsayed et al. [3], but no mathematical expression was provided. Stevens et al. [2] developed an enthalpy effectiveness expression analytically with Lewis factor being assumed as unity. In order to determine the outlet humidity ratio, an 'effective' heat and mass transfer process was assumed in which the solution stream was at a constant 'effective' temperature that gives the correct air outlet enthalpy. Allowing Lewis factor not necessarily equal to unity, Ren et al. [30] solved the differential equations for the coupled heat and mass transfer processes analytically. Expressions for the humidity and enthalpy effectiveness were further developed based on the analytical solution. However, both analytical models were based on the so called gas phase-controlled model. That is to say, liquid phase heat and mass transfer resistances were neglected.

Analytical solution can not only be helpful to compute the averaged heat and mass transfer coefficients from existing experimental data, it can also be very useful in annual energy performance analyses of liquid desiccant cooling and air conditioning systems and in optimization analyses and design calculations. Thus, this article is aimed at developing an analytical solution for the coupled heat and mass transfer processes, allowing both liquid and gas phase heat and mass transfer resistances not necessary equal to zero and Lewis factor not necessary equal to unity. Further, analytical expressions for the tower efficiency and other effectiveness values will be developed based on the analytical solution.

2. Physical model

The heat and mass transfer model for packed bed liquid desiccant–air contact systems can be schematically shown in Fig. 1. Due to the high surface tension of liquid solutions, the surface of packing materials may not be uniformly wetted. This will possibly lead to reduced areas for heat and mass transfer. Because of the fin effect of packing materials, the effective heat and mass transfer areas may not be equal. In order to improve model accuracy, a ratio of effective mass transfer area to the effective heat transfer area will be utilized to describe this effect. Also, Lewis factor for air phase will not be necessary set as unity even for the uniformly wetted conditions.

For modelling, the following assumptions are adopted as in conventional practices:

(1) zero wall and air thermal and moisture diffusivity in flow directions;
(2) no heat transfer to the surroundings;

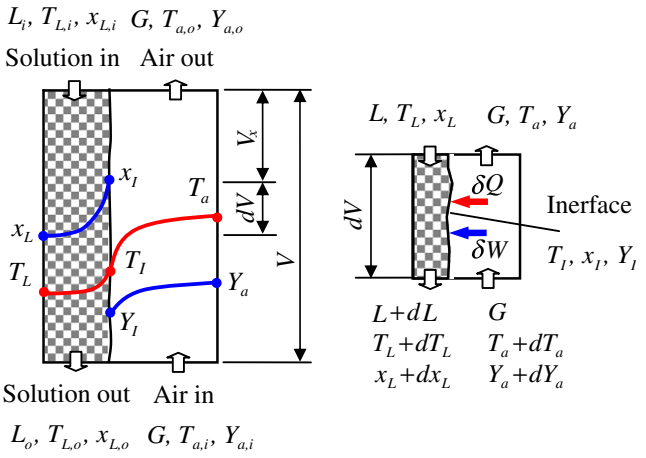

(a) Schematic of the exchanger (b) A differential element

Fig. 1. Double film mass transfer resistance model for liquid desiccant–air contact systems.

(3) constant specific heats of air and solution, constant heat and mass transfer coefficients and constant Lewis factor along the height of the exchanger.

3. Differential equations

For the differential element as shown in Fig. 1b, a set of differential equations can be obtained as follows:

Energy balance equation for air

$$G\,\mathrm{d}h_\mathrm{a} = \delta_\mathrm{a}[h_\mathrm{G}a(t_\mathrm{a}-t_\mathrm{I}) + h_{\mathrm{v,I}}k_Y a_M(Y_\mathrm{a}-Y_\mathrm{I})]\,\mathrm{d}V \tag{1}$$

Mass balance equation for air

$$G\,\mathrm{d}Y_\mathrm{a} = \delta_\mathrm{a}k_Y a_M(Y_\mathrm{a}-Y_\mathrm{I})\,\mathrm{d}V \tag{2}$$

Energy balance equation for the differential element

$$\mathrm{d}(Lh_\mathrm{L}) = \delta_\mathrm{a}G\,\mathrm{d}h_\mathrm{a} \tag{3}$$

Mass balance equation for the differential element

$$\mathrm{d}L = \frac{L}{1-x_\mathrm{L}}\,\mathrm{d}x_\mathrm{L} = \delta_\mathrm{a}G\,\mathrm{d}Y_\mathrm{a} \tag{4}$$

For desiccant solution, the Gibbs equation applies

$$\mathrm{d}(Lh_\mathrm{L}) = LC_\mathrm{L}\,\mathrm{d}t_\mathrm{L} + \hat{h}_\mathrm{w}\,\mathrm{d}L \tag{5}$$

Interface conditions are determined by the equations as follow:

Energy balance equation at interface

$$h_\mathrm{L}a(t_\mathrm{I}-t_\mathrm{L}) = h_\mathrm{G}a(t_\mathrm{a}-t_\mathrm{I}) + h_{\mathrm{s,I}}k_Y a_M(Y_\mathrm{a}-Y_\mathrm{I}) \tag{6}$$

Mass balance equation at interface

$$k_x a_M(x_\mathrm{I}-x_\mathrm{L}) = k_Y a_M(Y_\mathrm{a}-Y_\mathrm{I}) \tag{7}$$

Rearrange Eqs. (1)–(5) to give

$$\mathrm{d}t_\mathrm{a} = \delta_\mathrm{a}(t_\mathrm{a}-t_\mathrm{I})\frac{1}{B_1}\,\mathrm{dNTU} \tag{8}$$

$$\mathrm{d}Y_\mathrm{a} = \delta_\mathrm{a}(Y_\mathrm{a}-Y_\mathrm{I})(\sigma/Le_f)\,\mathrm{dNTU} \tag{9}$$

$$\mathrm{d}t_\mathrm{L} = \delta_\mathrm{a}C^*(B_0\,\mathrm{d}t_\mathrm{a} + B_2\bar{h}_{fg}\,\mathrm{d}Y_\mathrm{a}) \tag{10}$$

In above equations, $B_0 = (1+Y_\mathrm{a}R_\mathrm{cv}), B_1 = B_0/[1+R_\mathrm{cv}\frac{\sigma}{Le_f}(Y_\mathrm{I}-Y_\mathrm{a})]$ and $B_2 = (h_{\mathrm{v,a}}-\hat{h}_\mathrm{w})/h_{fg,0}$. The definitions of the other grouped parameters are defined as follow:

$\mathrm{NTU} = (h_\mathrm{G}aV)/(GC_{pa})$ and $\mathrm{dNTU} = (h_\mathrm{G}a\,\mathrm{d}V)/(GC_{pa})$—numbers of air side heat transfer units for the exchanger and the differential element, respectively;
$R_\mathrm{cv} = C_{pv}/C_{pa}$—water vapor to dry air specific heat capacity ratio;
$Le_f = h_\mathrm{G}/(k_Y C_{pa})$—Lewis factor for the gas phase heat and mass transfer;
$\sigma = a_M/a$—ratio of the effective mass transfer area to the effective heat transfer area;
$C^* = \frac{GC_{pa}}{LC_\mathrm{L}}$—air to solution heat capacity rate ratio;
$\bar{h}_{fg} = h_{fg,0}/C_{pa}$—a normalized heat of evaporation at reference condition (0 °C).

The total differential of equilibrium humidity ratio is

$$\mathrm{d}Y_\mathrm{e} = E_t\,\mathrm{d}t + E_x\,\mathrm{d}x \tag{11}$$

Here $E_t = \frac{\partial Y_\mathrm{e}}{\partial t}$ and $E_x = \frac{\partial Y_\mathrm{e}}{\partial x}$. Within relatively narrow range of operating conditions, the equilibrium humidity ratio of desiccant solution can be approximated as a linear function of concentration and temperature. With this approximation, Eq. (11) can be integrated from bulk solution to interface to give

$$Y_\mathrm{I} - Y_\mathrm{eL} = E_t(t_\mathrm{I}-t_\mathrm{L}) + E_x(x_\mathrm{I}-x_\mathrm{L}) \tag{12}$$

Substituting Eq. (7) into Eq. (12) gives

$$Y_\mathrm{I} - Y_\mathrm{eL} = E_t(t_\mathrm{I}-t_\mathrm{L}) + E_xR_k(Y_\mathrm{a}-Y_\mathrm{I}) \tag{13}$$

Here $R_k = k_Y/k_x$ represents the ratio of gas-to-liquid phase mass transfer coefficients. Solving Eqs. (6) and (13) simultaneously gives

$$Y_\mathrm{I} = \frac{1}{1+P_1}Y_\mathrm{eL} + \frac{P_1}{1+P_1}Y_\mathrm{a} + \frac{P_2}{1+P_1}\frac{t_\mathrm{a}-t_\mathrm{L}}{\bar{h}_{fg}} \tag{14}$$

$$t_\mathrm{I} = (1-P_3)t_\mathrm{L} + P_3t_\mathrm{a} + P_4\bar{h}_{fg}(Y_\mathrm{a}-Y_\mathrm{eL}) \tag{15}$$

Here

$$P_1 = E_xR_k + \frac{h_{\mathrm{s,I}}}{h_{fg,0}}\frac{\sigma}{Le_f}P_2$$

$$P_2 = E_t\bar{h}_{fg}\frac{R_h}{1+R_h}$$

$$P_3 = \frac{1+E_xR_k}{(1+P_1)E_t\bar{h}_{fg}}P_2$$

$$P_4 = \frac{P_1-E_xR_k}{(1+P_1)E_t\bar{h}_{fg}}$$

$$R_h = h_\mathrm{G}/h_\mathrm{L}$$

The following observations can be easily seen from the above expressions: if E_xR_k is much less than unity, the

effect of liquid phase mass transfer resistance can be neglected; if R_h is much less than unity, the effect of liquid phase heat transfer resistance can be neglected. Substitute Eqs. (14) and (15) into Eqs. (8) and (9) to give

$$\mathrm{d}t_\mathrm{a} = \delta_\mathrm{a}\frac{1}{B_1}[(1-P_3)(t_\mathrm{a}-t_\mathrm{L}) - P_4\bar{h}_{fg}(Y_\mathrm{a}-Y_\mathrm{eL})]\,\mathrm{dNTU} \tag{16}$$

$$\mathrm{d}Y_\mathrm{a} = \delta_\mathrm{a}\left[-\frac{P_2}{(1+P_1)\bar{h}_{fg}}(t_\mathrm{a}-t_\mathrm{L}) + \frac{1}{1+P_1}(Y_\mathrm{a}-Y_\mathrm{eL})\right]\frac{\sigma}{Le_f}\,\mathrm{dNTU} \tag{17}$$

Substituting Eq. (4) into Eq. (11) gives

$$\mathrm{d}Y_\mathrm{eL} = E_t\,\mathrm{d}t_\mathrm{L} + \delta_\mathrm{a}(1-x_\mathrm{L})m_\mathrm{R}E_x\,\mathrm{d}Y_\mathrm{a} \tag{18}$$

Here $m_\mathrm{R} = \frac{G}{L}$ represents the air to solution mass flow rate ratio.

Let's define dimensionless temperature as

$$\vartheta = t/\bar{h}_{fg} \tag{19}$$

Further define two new grouped parameters as

$$\Delta Y = Y_\mathrm{a} - Y_\mathrm{eL} \quad \text{and} \quad \Delta\vartheta = \vartheta_\mathrm{a} - \vartheta_\mathrm{L} \tag{20}$$

Using these definitions to rearrange Eq. (10) and Eqs. (16)–(18) gives a system of differential equations as

$$\frac{\mathrm{d}}{\mathrm{dNTU}}\mathbf{Y} = \mathbf{A}\mathbf{Y} \tag{21}$$

In this matrix equation, the variable vector $\mathbf{Y}$ represents the set of newly defined parameters as

$$\mathbf{Y} = (\Delta Y, \Delta\vartheta)^\mathrm{T} \tag{22}$$

and $\mathbf{A}$ represents the coefficients matrix

$$\mathbf{A} = (a_{ij})_{2\times2} = \begin{pmatrix} C^*S_\vartheta P_4\frac{B_0}{B_1} - \frac{B_3}{1+P_1}\frac{\sigma}{Le_f} & -C^*S_\vartheta(1-P_3)\frac{B_0}{B_1} + \frac{B_3P_2}{1+P_1}\frac{\sigma}{Le_f} \\ (C^*B_0-\delta_\mathrm{a})\frac{P_4}{B_1} - \frac{C^*B_2}{1+P_1}\frac{\sigma}{Le_f} & -(C^*B_0-\delta_\mathrm{a})\frac{1-P_3}{B_1} + \frac{C^*B_2P_2}{1+P_1}\frac{\sigma}{Le_f} \end{pmatrix} \tag{23}$$

Here $S_\vartheta = E_t\bar{h}_{fg}$ and $B_3 = -\delta_\mathrm{a} + C^*S_\vartheta B_2 + (1-x_\mathrm{L})m_\mathrm{R}E_x$. If liquid phase heat and mass transfer resistances are neglected, $P_1 = P_2 = P_3 = P_4 = 0$. The coefficients matrix will be reduced as

$$\mathbf{A} = (a_{ij})_{2\times2} = \begin{pmatrix} -B_3\frac{\sigma}{Le_f} & -C^*S_\vartheta\frac{B_0}{B_1} \\ -C^*B_2\frac{\sigma}{Le_f} & -(C^*B_0-\delta_\mathrm{a})\frac{1}{B_1} \end{pmatrix} \tag{24}$$

For the countercurrent flow configuration, this coefficients matrix is approximately equal to that developed in a previous article by Ren et al. in Ref. [30]. In effect, the parameter σ/Le_f in this article is equivalent to the parameter $1/Le$ in the previous article. In a_{11}, $-B_3$ is slightly different from $1 - C^*S_\vartheta$ in the previous article due to the different approximations in equilibrium humidity ratio of desiccant solutions. Other minor differences in a_{12}, a_{21} and a_{22} are due to the minor differences in the expressions of $\mathrm{d}t_\mathrm{L}$. Thus, this model can be considered as an extension of the previous model. However, the model can also be applied for much more complicated situations for both countercurrent and parallel flow configurations.

4. Analytical solution

Generally, all the elements in the coefficients matrix can be approximated as constants. From assumptions in Section 2, we can see that parameters σ/Le_f, R_h, R_k and $\bar{h}_{fg}$ are constants. Hence, the parameters P_1–P_4 can be taken as constants with the aforementioned linear approximation. The changes in mass flow rate and concentration of the desiccant solution are usually small and the values of these variables appeared in above equations can be evaluated as the averaged values. B_0, B_1 and B_2 are approximately equal to unity and can also be approximated as constants too. By above approximations, Eq. (23) represents a set of linear and homogeneous ordinary differential equations and can be solved analytically.

For Eq. (21), the characteristic equation is as follows

$$|\lambda\mathbf{E} - \mathbf{A}| = 0 \tag{25}$$

Within the practical range of operating conditions, numerical calculation shows that the solution of this characteristic equation will always give two different real roots. These roots are calculated as

$$\lambda_{1,2} = \left[(a_{11}+a_{22}) \pm \sqrt{(a_{11}+a_{22})^2 - 4(a_{11}a_{22}-a_{12}a_{21})}\right]/2 \tag{26}$$

Thus, analytical solution of Eq. (21) can be expressed as follows:

$$\Delta Y = C_1\mathrm{e}^{\lambda_1\mathrm{NTU}_x} + C_2\mathrm{e}^{\lambda_2\mathrm{NTU}_x} \tag{27}$$

$$\Delta\vartheta = -K_1C_1\mathrm{e}^{\lambda_1\mathrm{NTU}_x} + K_2C_2\mathrm{e}^{\lambda_2\mathrm{NTU}_x} \tag{28}$$

By satisfying the general solution of Eqs. (27) and (28) to Eq. (21), the constant coefficients K_1 and K_2 can be given as

$$K_1 = -(\lambda_1 - a_{11})/a_{12} \quad \text{and} \quad K_2 = (\lambda_2 - a_{11})/a_{12} \tag{29}$$

By satisfying Eqs. (23) and (28) to the top boundary conditions, i.e., for $\mathrm{NTU}_x = 0$, $\Delta Y = \Delta Y_\mathrm{T}$ and $\Delta\vartheta = \Delta\vartheta_\mathrm{T}$, we can get

$$C_1 = (K_2\Delta Y_\mathrm{T} - \Delta\vartheta_\mathrm{T})/(K_1+K_2) \tag{30}$$

$$C_2 = (K_1\Delta Y_\mathrm{T} + \Delta\vartheta_\mathrm{T})/(K_1+K_2) \tag{31}$$

For further simplification, another two new variables are defined as

$$\varphi = K_2 Y - \vartheta \quad \text{and} \quad \psi = K_1 Y + \vartheta \tag{32}$$

And the corresponding driving potentials are defined as

$$\begin{aligned}&\Delta\varphi = \varphi_{\mathrm{a}} - \varphi_{\mathrm{eL}} = K_2 \Delta Y - \Delta\vartheta \quad \text{and}\\ &\Delta\psi = \psi_{\mathrm{a}} - \psi_{\mathrm{eL}} = K_1 \Delta Y + \Delta\vartheta\end{aligned} \tag{33}$$

Substituting Eqs. (27) and (28) into Eq. (33) gives

$$\Delta\varphi = \Delta\varphi_{\mathrm{T}} \mathrm{e}^{\lambda_1 \mathrm{NTU}_x} \quad \text{and} \quad \Delta\psi = \Delta\psi_{\mathrm{T}} \mathrm{e}^{\lambda_2 \mathrm{NTU}_x} \tag{34}$$

From Eq. (34), the potential variables $\Delta\varphi$ and $\Delta\psi$ are seen to be decoupled from each other and are more convenient to use in calculation than the potential variables ΔY and $\Delta\vartheta$.

5. Effectiveness–NTU relation

Following Ren et al. [30], the humidity effectiveness (also known as tower efficiency) is defined as

$$\varepsilon_Y = \frac{Y_{\mathrm{a,i}} - Y_{\mathrm{a,o}}}{Y_{\mathrm{a,i}} - Y_{\mathrm{eL,i}}} \tag{35}$$

Similarly, the temperature and enthalpy effectiveness can be defined as

$$\varepsilon_t = \frac{t_{\mathrm{a,i}} - t_{\mathrm{a,o}}}{t_{\mathrm{a,i}} - t_{\mathrm{L,i}}} \quad \text{and} \quad \varepsilon_h = \frac{h_{\mathrm{a,i}} - h_{\mathrm{a,o}}}{h_{\mathrm{a,i}} - h_{\mathrm{eL,i}}} \tag{36}$$

Effectiveness for the new variables φ and ψ are defined as

$$\varepsilon_\varphi = \frac{\varphi_{\mathrm{a,i}} - \varphi_{\mathrm{a,o}}}{\varphi_{\mathrm{a,i}} - \varphi_{\mathrm{eL,i}}} \quad \text{and} \quad \varepsilon_\psi = \frac{\psi_{\mathrm{a,i}} - \psi_{\mathrm{a,o}}}{\psi_{\mathrm{a,i}} - \psi_{\mathrm{eL,i}}} \tag{37}$$

To develop analytical expressions for above effectiveness values, the following deduction processes are needed. Firstly, with linear approximation of the equilibrium humidity ratio, Eq. (11) can be further integrated from solution inlet to outlet to give

$$Y_{\mathrm{eL,o}} - Y_{\mathrm{eL,i}} = S_\vartheta(\vartheta_{\mathrm{L,o}} - \vartheta_{\mathrm{L,i}}) + E_x(x_{\mathrm{L,o}} - x_{\mathrm{L,i}}) \tag{38}$$

Due to the small changes in mass flow rate and concentration of the desiccant solution, Eq. (4) can be integrated approximately to give

$$x_{\mathrm{L,o}} - x_{\mathrm{L,i}} = [m_{\mathrm{R}}(1 - x_{\mathrm{L}})]_{\mathrm{av}}(Y_{\mathrm{a,i}} - Y_{\mathrm{a,o}}) \tag{39}$$

To satisfy overall mass balance condition, the average value $[m_{\mathrm{R}}(1 - x_{\mathrm{L}})]_{\mathrm{av}}$ can be evaluated as $G(1 - x_{\mathrm{L,o}})/L_i$. From Eqs. (32), (38) and (39), the following two equations can be obtained.

$$\begin{aligned}\varphi_{\mathrm{eL,o}} - \varphi_{\mathrm{eL,i}} &= (K_2 S_\vartheta - 1)(\vartheta_{\mathrm{L,o}} - \vartheta_{\mathrm{L,i}})\\ &\quad + K_2 E_x [m_{\mathrm{R}}(1 - x_{\mathrm{L}})]_{\mathrm{av}}(Y_{\mathrm{a,i}} - Y_{\mathrm{a,o}})\end{aligned} \tag{40}$$

$$\begin{aligned}\psi_{\mathrm{eL,o}} - \psi_{\mathrm{eL,i}} &= (K_1 S_\vartheta + 1)(\vartheta_{\mathrm{L,o}} - \vartheta_{\mathrm{L,i}})\\ &\quad + K_1 E_x [m_{\mathrm{R}}(1 - x_{\mathrm{L}})]_{\mathrm{av}}(Y_{\mathrm{a,i}} - Y_{\mathrm{a,o}})\end{aligned} \tag{41}$$

Eq. (10) can be rewritten in a dimensionless form as follows:

$$\mathrm{d}\vartheta_{\mathrm{L}} = \delta_{\mathrm{a}} C^*(B_0\,\mathrm{d}\vartheta_{\mathrm{a}} + B_2\,\mathrm{d}Y_{\mathrm{a}}) \tag{42}$$

Integrating Eq. (42) from solution inlet to outlet to give

$$\vartheta_{\mathrm{L,o}} - \vartheta_{\mathrm{L,i}} = C^*[B_0(\vartheta_{\mathrm{a,i}} - \vartheta_{\mathrm{a,o}}) + B_2(Y_{\mathrm{a,i}} - Y_{\mathrm{a,o}})] \tag{43}$$

Substituting Eq. (43) into Eqs. (40) and (41) gives the following equations:

$$\begin{aligned}\varphi_{\mathrm{eL,o}} - \varphi_{\mathrm{eL,i}} &= (K_2 S_\vartheta - 1) C^* B_0(\vartheta_{\mathrm{a,i}} - \vartheta_{\mathrm{a,o}}) + \{(K_2 S_\vartheta - 1) C^* B_2\\ &\quad + K_2 E_x [m_{\mathrm{R}}(1 - x_{\mathrm{L}})]_{\mathrm{av}}\}(Y_{\mathrm{a,i}} - Y_{\mathrm{a,o}})\end{aligned} \tag{44}$$

$$\begin{aligned}\psi_{\mathrm{eL,o}} - \psi_{\mathrm{eL,i}} &= (K_1 S_\vartheta + 1) C^* B_0(\vartheta_{\mathrm{a,i}} - \vartheta_{\mathrm{a,o}}) + \{(K_1 S_\vartheta + 1) C^* B_2\\ &\quad + K_1 E_x [m_{\mathrm{R}}(1 - x_{\mathrm{L}})]_{\mathrm{av}}\}(Y_{\mathrm{a,i}} - Y_{\mathrm{a,o}})\end{aligned} \tag{45}$$

Humidity ratio Y and dimensionless temperature ϑ can be expressed in terms of variables φ and ψ by solving Eq. (32) as follows:

$$\begin{aligned}&Y = (\varphi + \psi)/(K_1 + K_2) \quad \text{and}\\ &\vartheta = (K_2\psi - K_1\varphi)/(K_1 + K_2)\end{aligned} \tag{46}$$

Substituting Eq. (46) into Eqs. (44) and (45) gives the following equations:

$$\varphi_{\mathrm{eL,o}} - \varphi_{\mathrm{eL,i}} = \beta_1(\varphi_{\mathrm{a,i}} - \varphi_{\mathrm{a,o}}) + \beta_2(\psi_{\mathrm{a,i}} - \psi_{\mathrm{a,o}}) \tag{47}$$

$$\psi_{\mathrm{eL,o}} - \psi_{\mathrm{eL,i}} = \beta_3(\varphi_{\mathrm{a,i}} - \varphi_{\mathrm{a,o}}) + \beta_4(\psi_{\mathrm{a,i}} - \psi_{\mathrm{a,o}}) \tag{48}$$

where the coefficients β's are calculated as

$$\beta_1 = C^*(K_2 S_\vartheta - 1)\frac{B_2 - K_1 B_0}{K_1 + K_2} + \frac{K_2}{K_1 + K_2} E_x [m_{\mathrm{R}}(1 - x_{\mathrm{L}})]_{\mathrm{av}} \tag{49}$$

$$\beta_2 = C^*(K_2 S_\vartheta - 1)\frac{B_2 + K_2 B_0}{K_1 + K_2} + \frac{K_2}{K_1 + K_2} E_x [m_{\mathrm{R}}(1 - x_{\mathrm{L}})]_{\mathrm{av}} \tag{50}$$

$$\beta_3 = C^*(K_1 S_\vartheta + 1)\frac{B_2 - K_1 B_0}{K_1 + K_2} + \frac{K_1}{K_1 + K_2} E_x [m_{\mathrm{R}}(1 - x_{\mathrm{L}})]_{\mathrm{av}} \tag{51}$$

$$\beta_4 = C^*(K_1 S_\vartheta + 1)\frac{B_2 + K_2 B_0}{K_1 + K_2} + \frac{K_1}{K_1 + K_2} E_x [m_{\mathrm{R}}(1 - x_{\mathrm{L}})]_{\mathrm{av}} \tag{52}$$

Next, Eq. (34) can be rewritten as follows. For countercurrent flow configuration

$$\begin{aligned}&(\varphi_{\mathrm{a,i}} - \varphi_{\mathrm{eL,i}}) - (\varphi_{\mathrm{eL,o}} - \varphi_{\mathrm{eL,i}})\\ &\quad = [(\varphi_{\mathrm{a,i}} - \varphi_{\mathrm{eL,i}}) - (\varphi_{\mathrm{a,i}} - \varphi_{\mathrm{a,o}})]\mathrm{e}^{\lambda_1 \mathrm{NTU}}\end{aligned} \tag{53}$$

$$\begin{aligned}&(\psi_{\mathrm{a,i}} - \psi_{\mathrm{eL,i}}) - (\psi_{\mathrm{eL,o}} - \psi_{\mathrm{eL,i}})\\ &\quad = [(\psi_{\mathrm{a,i}} - \psi_{\mathrm{eL,i}}) - (\psi_{\mathrm{a,i}} - \psi_{\mathrm{a,o}})]\mathrm{e}^{\lambda_2 \mathrm{NTU}}\end{aligned} \tag{54}$$

For parallel flow configuration

$$\begin{aligned}&(\varphi_{\mathrm{a,i}} - \varphi_{\mathrm{eL,i}}) - (\varphi_{\mathrm{a,i}} - \varphi_{\mathrm{a,o}}) - (\varphi_{\mathrm{eL,o}} - \varphi_{\mathrm{eL,i}})\\ &\quad = (\varphi_{\mathrm{a,i}} - \varphi_{\mathrm{eL,i}})\mathrm{e}^{\lambda_1 \mathrm{NTU}}\end{aligned} \tag{55}$$

$$\begin{aligned}&(\psi_{\mathrm{a,i}} - \psi_{\mathrm{eL,i}}) - (\psi_{\mathrm{a,i}} - \psi_{\mathrm{a,o}}) - (\psi_{\mathrm{eL,o}} - \psi_{\mathrm{eL,i}})\\ &\quad = (\psi_{\mathrm{a,i}} - \psi_{\mathrm{eL,i}})\mathrm{e}^{\lambda_2 \mathrm{NTU}}\end{aligned} \tag{56}$$

Finally, substitute Eqs. (47) and (48) into Eqs. (53) and (54) and solve the resultant equations to give the expressions for

the effectiveness values of φ and ψ in counterflow configuration as

$$\varepsilon_\varphi = \frac{\beta_2\gamma(1-e^{\lambda_2 NTU}) - (\beta_4 - e^{\lambda_2 NTU})(1-e^{\lambda_1 NTU})}{\beta_2\beta_3 - (\beta_1 - e^{\lambda_1 NTU})(\beta_4 - e^{\lambda_2 NTU})} \quad (57)$$

$$\varepsilon_\psi = \frac{\beta_3(1-e^{\lambda_1 NTU})/\gamma - (\beta_1 - e^{\lambda_1 NTU})(1-e^{\lambda_2 NTU})}{\beta_2\beta_3 - (\beta_1 - e^{\lambda_1 NTU})(\beta_4 - e^{\lambda_2 NTU})} \quad (58)$$

Substitute Eqs. (47) and (48) into Eqs. (55) and (56) and solve the resultant equations to give the expressions for the effectiveness values of φ and ψ in parallel flow configuration as

$$\varepsilon_\varphi = \frac{(1+\beta_4)(1-e^{\lambda_1 NTU}) - \beta_2\gamma(1-e^{\lambda_2 NTU})}{(1+\beta_1)(1+\beta_4) - \beta_2\beta_3} \quad (59)$$

$$\varepsilon_\psi = \frac{(1+\beta_1)(1-e^{\lambda_2 NTU}) - \beta_3/\gamma(1-e^{\lambda_1 NTU})}{(1+\beta_1)(1+\beta_4) - \beta_2\beta_3} \quad (60)$$

Here, coefficient γ is defined as

$$\gamma = (\psi_{a,i} - \psi_{eL,i})/(\varphi_{a,i} - \varphi_{eL,i}) \quad (61)$$

From Eq. (46), tower efficiency and temperature effectiveness can be expressed as

$$\varepsilon_Y = \frac{\varepsilon_\varphi + \gamma\varepsilon_\psi}{1+\gamma} \quad \text{and} \quad \varepsilon_t = \varepsilon_\vartheta = \frac{K_2\gamma\varepsilon_\varphi - K_1\varepsilon_\psi}{K_2\gamma - K_1} \quad (62)$$

Enthalpy effectiveness can be expressed as

$$\varepsilon_h = \frac{(B_{41} - K_1B_{01})\varepsilon_\varphi + (B_{41} + K_2B_{01})\gamma\varepsilon_\psi}{(B_{42} - K_1B_{01}) + (B_{42} + K_2B_{01})\gamma} \quad (63)$$

Here, $B_{01} = 1 + Y_{a,i}R_{cv}$, $B_{41} = 1 + R_{cv}\vartheta_{a,o}$ and $B_{42} = 1 + R_{cv}\vartheta_{L,i}$.

6. Calculation procedure

In rating calculation, outlet parameters have to be determined. With a given set of inlet conditions and control parameters $(t_{L,i}, t_{a,i}, x_{L,i}, Y_{a,i}, C_i^* = \frac{GC_{pa}}{(LC_L)_i}, R_k, R_h, \sigma/Le_f$ and NTU), the values of coefficients and parameters B_0–B_4, E_t, E_x, C^* and P_1–P_4 have to be evaluated at first for an analytical solution. In evaluating the values of B_0–B_3, C^*, P_1 and P_4, the arithmetic mean values of temperatures, concentrations and humidity ratios at the inlet and outlet positions are used. The coefficients E_t and E_x are evaluated according to the following equations:

$$E_t = (Y_{eL}(t_{L,i}, x_{L,i}) + Y_{eL}(t_{L,i}, x_{L,o}) - Y_{eL}(t_{L,o}, x_{L,i}) - Y_{eL}(t_{L,o}, x_{L,o}))/[2(t_{L,i} - t_{L,o})] \quad (64)$$

$$E_x = (Y_{eL}(t_{L,i}, x_{L,i}) + Y_{eL}(t_{L,o}, x_{L,i}) - Y_{eL}(t_{L,i}, x_{L,o}) - Y_{eL}(t_{L,o}, x_{L,o}))/[2(x_{L,i} - x_{L,o})] \quad (65)$$

For above evaluations, outlet parameters $x_{L,o}$ and $t_{L,o}$ are calculated according to Eqs. (39) and (43), respectively, after analytical results of $Y_{a,o}$ and $t_{a,o}$ have been obtained. Interface parameters are calculated according to Eqs. (7), (14) and (15).

Because evaluation results also depend on outlet parameters, iterative processes will be required. Usually, 3–5 steps are needed for an analytical solution. Initially, the values of outlet temperatures, concentration and humidity ratio are simply assumed as their inlet values, respectively. E_x and E_t are evaluated according to their differential expressions at the inlet positions too. Though this is rather arbitrarily an evaluation, it will not affect the final results of the iteration solution.

Based on above conditions and specifications, a procedure for the analytical solution is given as follows:

(1) Evaluate the values of coefficients and parameters B_0–B_4, E_t, E_x, C^* and P_1–P_4 based on given conditions and initially assumed or iterative results of outlet parameters.
(2) Calculate values of the elements of coefficients matrix **A** according to Eq. (23).
(3) Calculate the roots of the characteristic equation according to Eq. (26).
(4) Calculate coefficients K_1 and K_2 according to Eq. (29).
(5) Calculate β_1–β_4 according to Eqs. (49)–(52).
(6) Calculate effectiveness values according to Eqs. (57)–(63).
(7) Calculate outlet parameters such as $Y_{a,o}$, $t_{a,o}$ and $h_{a,o}$ from effectiveness values.
(8) Check if the calculated outlet parameters match with the assumed values or the results of the last iteration and repeat steps (1)–(7) until the errors are acceptable.

7. Comparison and discussion

For counterflow configuration, the effectiveness expressions developed in this article are very similar to those developed in the previous article [30] (where there were some misprints and the corrections are listed in Appendix A). If liquid phase heat and mass transfer resistances can be neglected, β_1–β_4 will be approximately equal to B_1–B_4 in the previous article, respectively. Thus, the effectiveness expressions of φ and ψ are approximately equal in both articles, respectively. However, the effectiveness expression for enthalpy is improved for accuracy.

In developing analytical solution, approximations of linear equilibrium humidity ratio and constant values of variables involved in calculating the elements of the coefficients matrix **A** were adopted. These approximations will certainly introduce some errors in the analytical results. In order to demonstrate the validity of the analytical solution, comparisons were made between analytical and numerical results for some typical operating conditions. In comparison, a base case condition was selected for the LiCl solution based dehumidification as shown in Table 1. Other conditions were obtained by changing each time one independent variable from low to high values within typical ranges of operating conditions. For regeneration, the equipment operates at high desiccant solution temperature

Table 1
Comparison of analytical and numerical results for packed bed liquid desiccant air contact systems

Given conditions											This model			Previous model [30]			Numerical integration			[a]Relative errors (%) for			
Solution	[b]Flow type	$t_{L,i}$, °C	$x_{L,i}(\xi_{L,i})$, %	$t_{a,i}$, °C	$Y_{a,i}$, mol/mol(a)	C_i[b]	R_k	R_h	$\frac{\sigma}{Le_f}$	NTU	$t_{L,o}$, °C	$t_{a,o}$, °C	$Y_{a,o}$, mol/mol(a)	$t_{L,o}$, °C	$t_{a,o}$, °C	$Y_{a,o}$, mol/mol(a)	$t_{L,o}$, °C	$t_{a,o}$, °C	$Y_{a,o}$, mol/mol(a)	This model		Previous model	
																				e_{t_L}	e_Y	e_{t_L}	e_Y
LiCl	C	30	81.38(35)	35	0.03464	0.25	3	0	1	3	37.44	32.03	0.01794	38.4	32.02	0.01552	37.45	32.11	0.01787	−0.13	−0.42	12.75	14.01
LiCl	C	30	81.38(35)	35	0.03464	0.25	3	0	1	1	34.42	33.03	0.02493	35.51	33.26	0.02203	34.34	33.03	0.02514	1.84	2.21	26.96	32.74
LiCl	C	30	81.38(35)	35	0.03464	0.25	3	0	1	10	39.62	30.39	0.01344	39.88	30.23	0.01286	39.73	30.35	0.01317	−1.13	−1.26	1.54	1.44
LiCl	C	30	81.38(35)	35	0.03464	0.25	3	0	0.5	3	35.74	31.76	0.02241	36.87	31.97	0.01942	35.68	31.80	0.02256	1.06	1.24	20.95	25.99
LiCl	C	30	81.38(35)	35	0.03464	0.25	3	0	1.5	3	38.28	32.03	0.01581	39.01	31.86	0.01406	38.35	32.11	0.01559	−0.84	−1.15	7.90	8.03
LiCl	C	30	81.38(35)	35	0.03464	0.25	3	0.3	1	3	36.32	34.05	0.01950	38.4	32.02	0.01552	36.18	34.15	0.01979	2.27	1.95	35.92	28.75
LiCl	C	30	81.38(35)	35	0.03464	0.25	9	0	1	3	36.12	31.84	0.02140	38.4	32.02	0.01552	35.92	31.89	0.02188	3.38	3.76	41.89	49.84
LiCl	C	30	81.38(35)	35	0.03464	0.25	0	0	1	3	38.41	32.01	0.01550	38.4	32.02	0.01552	38.50	31.99	0.01526	−1.06	−1.24	−1.18	−1.34
LiCl	C	30	81.38(35)	35	0.03464	0.125	3	0	1	3	34.16	31.05	0.01652	34.6	30.97	0.01435	34.14	31.06	0.01658	0.48	0.33	11.11	12.35
LiCl	C	30	81.38(35)	35	0.03464	0.5	3	0	1	3	41.14	34.26	0.02110	42.42	34.82	0.01909	41.12	34.56	0.02092	0.18	−1.31	11.69	13.34
LiCl	C	30	81.38(35)	35	0.05288	0.25	3	0	1	3	42.09	33.34	0.02346	43.99	33.45	0.01847	42.09	33.6	0.02330	0.00	−0.54	15.72	16.33
LiCl	C	30	81.38(35)	35	0.01702	0.25	3	0	1	3	32.42	30.76	0.01371	32.59	30.76	0.01327	32.42	30.77	0.01369	0.00	−0.60	7.02	12.61
LiCl	C	30	81.38(35)	27	0.03464	0.25	3	0	1	3	35.81	31.27	0.01739	36.73	31.21	0.01509	35.77	31.34	0.01743	0.69	0.23	16.64	13.60
LiCl	C	30	81.38(35)	45	0.03464	0.25	3	0	1	3	39.45	32.98	0.01871	40.45	33.05	0.01612	39.54	33.08	0.01843	−0.94	−1.73	9.54	14.25
LiCl	C	30	77.92(40)	35	0.03464	0.25	3	0	1	3	39.49	32.33	0.01313	40.39	32.24	0.01095	39.48	32.45	0.01308	0.11	−0.23	9.60	9.88
LiCl	C	30	98.72(5)	35	0.03464	0.25	3	0	1	3	29.15	29.96	0.04037	28.95	29.96	0.04089	29.16	29.96	0.04034	1.19	0.53	25.00	9.65
LiCl	C	15	81.38(35)	35	0.03464	0.25	3	0	1	3	29.21	18.83	0.00941	29.94	18.72	0.00764	29.35	18.92	0.009	−0.98	−1.60	4.11	5.30
LiCl	C	55	81.38(35)	35	0.03464	0.15	3	0	1	3	49.88	52.77	0.04436	48.82	52.46	0.04894	49.91	52.79	0.04426	0.59	1.04	21.41	48.65
LiCl	P	30	81.38(35)	35	0.03464	0.25	3	0	1	3	35.84	35.20	0.01998				35.80	35.18	0.02009	0.69	0.76		
LiBr	C	15	82.82(50)	35	0.03464	0.25	3	0	1	3	28.83	18.68	0.00897	29.63	18.59	0.00686	28.91	18.82	0.00866	−0.58	−1.19	5.18	6.93
LiBr	C	55	82.82(50)	35	0.03464	0.15	3	0	1	3	50.92	53.11	0.04028	50.2	52.87	0.04371	50.93	53.1	0.04026	0.25	0.36	17.94	61.39
LiBr	C	15	82.82(50)	35	0.03464	0.25	3	0.3	1	3	24.27	20.69	0.00797	29.63	18.59	0.00686	24.17	20.90	0.00811	0.25	0.36	17.94	61.39
LiBr	P	15	82.82(50)	35	0.03464	0.25	3	0	1	3	26.29	25.53	0.01125				26.19	25.62	0.01144	−0.35	0.82		
$CaCl_2$	C	15	91.96(35)	35	0.03464	0.25	3	0	1	3	26.64	18.59	0.01519	27.72	18.6	0.01231	26.84	18.71	0.01459	−1.69	−2.99	7.43	11.37
$CaCl_2$	C	55	91.96(35)	35	0.03464	0.15	3	0	1	3	46.69	51.69	0.05913	41.93	50.07	0.0802	46.55	51.77	0.05965	−1.66	−2.08	54.67	82.17
$CaCl_2$	C	15	91.96(35)	35	0.03464	0.25	3	0.3	1	3	25.06	21.78	0.01731	27.72	18.6	0.01231	24.90	22.02	0.01757	−0.53	1.52	−9.37	30.81
$CaCl_2$	P	15	91.96(35)	35	0.03464	0.25	3	0	1	3	24.24	23.97	0.01803				24.23	24.00	0.01806	−0.03	0.18		

[a] Definitions for relative errors: $e_{t_L} = (t^n_{L,o} - t^a_{L,o})/(t_{L,i} - t^n_{L,o}), e_Y = (Y^n_{a,o} - Y^a_{a,o})/(Y_{a,i} - Y^n_{a,o})$.
[b] *C*—counterflow, *P*—parallel flow.

conditions. The minimum flow rates of desiccant solutions required by equilibrium calculation under these conditions are much higher than those at low temperature operating conditions. And thus, a lower value of air to solution heat capacity rate ratio C_i^* was selected for regeneration cases. From heat and mass transfer analogy, $h_G = F_G M_G C_G \left(\frac{Sc_G}{Pr_G}\right)^{2/3}$ and $h_L = F_L M_L C_L \left(\frac{Sc_L}{Pr_L}\right)^{2/3}$ [20]. Thus, we may have $\frac{R_h}{R_k} \approx \frac{M_G C_G}{(1-x_M) M_L C_G} \left(\frac{Sc_G}{Pr_G} / \frac{Sc_L}{Pr_L}\right)^{2/3}$. This may not be an exact correlation, but it can be a good estimation of the order of the magnitude of $\frac{R_h}{R_k}$. For typical operating conditions, $\frac{R_h}{R_k}$ will be in the order of 0.05–0.1 due to the large values of $\frac{Sc_L}{Pr_L}$ of liquid desiccant solutions. For simplicity, only three cases of dehumidification and one case of regeneration was selected for comparison for both the LiBr and $CaCl_2$ solutions based systems. In calculation, thermo-physical properties of desiccant solutions were obtained from literatures [15,31–33].

Results of outlet temperatures and humidity ratios from both analytical method and numerical integration are shown in Table 1 for comparison. For the typical operating conditions simulated, the differences are generally small. The differences in solution outlet temperatures are less than 0.2 °C and averagely equal to 0.073 °C. The differences in air outlet temperatures are less than 0.3 °C and averagely equal to 0.086 °C. The differences in air outlet humidity ratios are less than 0.0006 mol/mol(a) (or 0.375 g/kg(a)) and averagely equal to 0.0002 mol/mol(a) (or 0.13 g/kg(a)). Relative errors in outlet solution temperatures and air humidity ratios were also defined and calculated. These errors were defined as the ratios of the differences between the predicted outlet variable values by numerical integration and the analytical method respectively to the overall changes of the same variables by numerical integration. By the way of these definitions, relative errors in outlet air humidity ratios are also the relative errors in tower efficiency or latent energy exchanged. In addition, the total energy exchanged is approximately proportional to the overall change of desiccant solution temperatures and thus the relative errors in outlet solution temperatures approximately represent the relative errors in total energy exchanged. Due to the possibly zero values of overall changes in air temperatures, relative errors in air temperatures were not defined and calculated. However, the model accuracy can be adequately described by the relative errors in total and latent energy exchanged. It can be found from Table 1 that the relative errors are generally small for the typical operating conditions simulated. The absolute values of relative errors in outlet solution temperatures are less than 3.38% and averagely equal to 0.85%. For outlet air humidity ratios, the absolute values of relative errors are less than 3.76% and averagely equal to 1.18%.

Results of outlet temperatures and humidity ratios by a previous analytical method [30] are also shown in Table 1 for comparison. This method was based on a single film of gas phase heat and mass transfer resistance model. The comparison shows that the improvement in accuracy by the present analytical method over the previous one is significant. In real applications, the relative errors by the previous analytical method will not be so much great as shown in Table 1 if overall heat and mass transfer coefficients based on the same analytical method are utilized. Nonetheless, the present analytical model is more reasonable than the previous one and gives more detailed information on the complicated heat and mass transfer processes for the cases with non-negligible liquid phase mass transfer resistances.

By above comparisons, the validity of the present model is demonstrated to be satisfactory. However, additional simulations (not shown in Table 1) indicate that the relative errors increase with much larger values of air to solution heat capacity rate ratio C_i^* especially at higher temperature operating conditions. This is due to the increased nonlinearity of equilibrium humidity ratio of desiccant solutions. Further improvement could be obtained by taking into analytical solution the effect of nonlinearity of equilibrium humidity ratio of the desiccant solutions.

Appendix A. Corrections to the misprints in Ref. [30]

Misprinted equation No.	Corrected equation
(14)	$\mathrm{d}T_L = C^*[(T_a - T_L) + (\bar{h}_s/Le)(Y_a - Y_{eL})]\mathrm{dNTU}$
(22)	$a_{22} = \frac{Le - R_{cv}(Y_a - Y_{eL})}{Le(1+Y_a R_{cv})} - C^*$
(39)	$\vartheta_{L,o} - \vartheta_{L,i} = C^* \left\{ \frac{(R_{cv}(\vartheta_a - \vartheta_L) + 1)_{av} - K_1(1 + Y_a R_{cv})_{av}}{K_1 + K_2} \varepsilon_\varphi (\varphi_{a,i} - \varphi_{eL,i}) + \frac{(R_{cv}(\vartheta_a - \vartheta_L)+1)_{av} + K_2(1+Y_a R_{cv})_{av}}{K_1+K_2} \varepsilon_\psi (\psi_{a,i} - \psi_{eL,i}) \right\}$
(43)	$B_2 = C^*(K_2 S_\vartheta - 1) \frac{(R_{cv}(\vartheta_a - \vartheta_L)+1)_{av} + K_2(1+Y_a R_{cv})_{av}}{K_1+K_2}$
(45)	$B_4 = C^*(K_1 S_\vartheta + 1) \frac{(R_{cv}(\vartheta_a - \vartheta_L)+1)_{av} + K_2(1+Y_a R_{cv})_{av}}{K_1+K_2}$
(50)	$\varepsilon_h = \frac{h_{a,i} - h_{a,o}}{h_{a,i} - h_{eL,i}} = \frac{(\gamma_h - K_1)\varepsilon_\varphi + (K_2 + \gamma_h)\gamma \varepsilon_\psi}{(\gamma_h - K_1) + (K_2 + \gamma_h)\gamma}$

References

[1] H.M. Factor, G. Grossman, A packed bed dehumidifier/regenerator for solar air conditioning with liquid desiccants, Solar Energy 24 (1980) 541–550.

[2] D.I. Stevens, J.E. Braun, S.A. Klein, An effectiveness model of liquid-desiccant system heat/mass exchangers, Solar Energy 42 (6) (1989) 449–455.

[3] M.M. Elsayed, H.N. Gari, A.M. Radhwan, Effectiveness of heat and mass transfer in packed beds of liquid desiccant systems, Renewab. Energy 3 (6/7) (1993) 661–668.

[4] P. Gandhidasan, M.R. Ullah, C.F. Kettleborough, Analysis of heat and mass transfer between a desiccant–air system in a packed tower, J. Solar Energy Eng. 109 (1987) 89–93.

[5] V. Oberg, D.Y. Goswami, Experimental study of the heat and mass transfer in a packed bed liquid desiccant air dehumidifier, J. Solar Energy Eng. 120 (1998) 289–297.

[6] V. Martin, D.Y. Goswami, Heat and mass transfer in packed bed liquid desiccant regenerators—An experimental investigation, J. Solar Energy Eng. 121 (1999) 162–170.
[7] K. Onda, H. Takeuchi, Y. Okumoto, Mass transfer coefficients between gas and liquid phase in packed columns, J. Chem. Eng. Jpn. 1 (1968) 56–62.
[8] N. Fumo, D.Y. Goswami, Study of an aqueous lithium chloride desiccant system: air dehumidification and desiccant regeneration, Solar Energy 72 (4) (2002) 351–361.
[9] P. Gandhidasan, C.F. Kettleborough, M.R. Ullah, Calculation of heat and mass transfer coefficients in a packed tower operating with a desiccant–air contact system, J. Solar Energy Eng. 108 (1986) 123–128.
[10] A. Ertas, E.E. Anderson, S. Kavasogullari, Comparison of mass and heat-transfer coefficients of liquid-desiccant mixtures in a packed-column, J. Energy Resour. Technol. 113 (1) (1991) 1–6.
[11] R.E. Treybal, Mass-Transfer Operations, third ed., McGraw-Hill, New York, 1980, pp. 186–211.
[12] T.W. Chung, T.K. Ghosh, A.L. Hines, Comparison between random and structured packings for dehumidification of air by lithium chloride solutions in a packed column and their heat and mass transfer correlations, Indus. Eng. Chem. Res. 35 (1996) 192–198.
[13] T.W. Chung, H. Wu, Mass transfer correlation for dehumidification of air in a packed absorber with an inverse U-shaped tunnel, Separat. Sci. Technol. 35 (10) (2000) 1503–1515.
[14] T.W. Chung, T.K. Ghosh, A.L. Hines, Dehumidification of air by aqueous lithium chloride in a packed column, Separat. Sci. Technol. 28 (1–3) (1993) 533–550.
[15] S.V. Potnis, T.G. Lenz, Dimensionless mass-transfer correlations for packed-bed liquid desiccant contactors, Indust. Eng. Chem. Res. 35 (1996) 4185–4193.
[16] J.L. Bravo, J.A. Rocha, J.R. Fair, Mass transfer in gauze packings, Hydrocarbon Process. 64 (1) (1985) 91–95.
[17] J.L. Bravo, J.A. Rocha, J.R. Fair, Pressure drop in structured packings, Hydrocarbon Process. 56 (3) (1986) 45–59.
[18] J.A. Rocha, J.L. Bravo, J.R. Fair, Distillation columns containing structured packings. A comprehensive model for their performance. 1. Hydraulic models, Indus. Eng. Chem. Res. 32 (1993) 641–651.
[19] J.A. Rocha, J.L. Bravo, J.R. Fair, Distillation columns containing structured packings. A comprehensive model for their performance. 2. Mass transfer model, Indus. Eng. Chem. Res. 35 (1996) 1660–1667.
[20] A.A. Al-Farayedhi, P. Gandhidasan, M.A. Al-Mutairi, Evaluation of heat and mass transfer coefficients in a gauze-type structured packing air dehumidifier operating with liquid desiccant, Int. J. Refrigerat. 25 (2002) 330–339.
[21] R.H. Weiland, K.R. Ahlgren, Mass-transfer characteristics of some structured packings, Indus. Eng. Chem. Res. 32 (1993) 1411–1418.
[22] E. Brunazzi, A. Paglianti, Liquid-film mass transfer coefficient in a column equipped with structured packings, Indus. Eng. Chem. Res. 36 (1997) 3792–3799.
[23] P.A. Nawrocki, K.T. Chuang, Carbon dioxide absorption into a stable liquid rivulet, Canad. J. Chem. Eng. 74 (1996) 247–255.
[24] S. Piche, B.P.A. Grandjean, I. Iliuta, F. Larachi, interfacial mass transfer in randomly packed towers: a confident correlation for environmental applications, Environ. Sci. Technol. 35 (2001) 4817–4822.
[25] M. Park, J.R. Howell, G.C. Vliet, Correlations for film regeneration and air dehumidification for a falling desiccant film with air in crossflow, J. Heat Transfer 118 (1996) 634–641.
[26] S. Patnaik, T.G. Lenz, G.O.G. Lof, Performance studies for an experimental solar open-cycle liquid desiccant air dehumidification system, Solar Energy 44 (3) (1990) 123–135.
[27] M.R. Ullah, C.F. Kettleborough, P. Gandhidasan, Effectiveness of moisture removal for an adiabatic counterflow packed tower absorber operating with $CaCl_2$–air contact system, J. Solar Energy Eng. 110 (1988) 98–101.
[28] T.W. Chung, Predictions of the moisture removal efficiencies for packed bed dehumidification systems, Gas Separat. Purif. 8 (4) (1994) 265–268.
[29] V. Martin, D.Y. Goswami, Effectiveness of heat and mass transfer processes in a packed bed liquid desiccant dehumidifier/regenerator, HVAC&R Res. 6 (1) (2000) 21–39.
[30] C.Q. Ren, Y. Jiang, Y.P. Zhang, Simplified analysis of coupled heat and mass transfer processes in packed bed liquid desiccant–air contact system, Solar Energy 80 (1) (2006) 121–131.
[31] M.R. Patterson, H. Perez-Blanco, Numerical fits of the properties of lithium-bromide water solutions, ASHRAE Trans. 96 (2) (1988) 2059–2077.
[32] M.R. Conde, Properties of aqueous solutions of lithium and calcium chlorides: formulations for use in air conditioning equipment design, Int. J. Thermal Sci. 43 (4) (2004) 367–382.
[33] R. Manuel, Aqueous solutions of lithium and calcium chloride: property formulations for use in air conditioning equipment design, M. Conde Engineering ZurichSwitzerland, Univ of Zurich, Zurrch-Swizerland, 2002, pp. 1–26.